

CONFIDENTIAL

JAN 11 1989

Los Alamos National Laboratory is operated by the University of California for the United States Department of Energy under contract W-7405-ENG-36

LA-UR--87-4002

MASTER

DE88 004321

TITLE A CHEMICAL PRECURSOR TO OPTICAL DAMAGE?
STUDIES BY LASER IONIZATION MASS SPECTROMETRY

AUTHOR(S) N. S. Nogar and R. C. Estler

SUBMITTED TO 1987 Boulder Damage Symposium

DISCLAIMER

This report was prepared as an account of work sponsored by an agency of the United States Government. Neither the United States Government nor any agency thereof, nor any of their employees, makes any warranty, express or implied, or assumes any legal liability or responsibility for the accuracy, completeness, or usefulness of any information, apparatus, product, or process disclosed, or represents that its use would not infringe privately owned rights. Reference herein to any specific commercial product, process, or service by trade name, trademark, manufacturer, or otherwise does not necessarily constitute or imply its endorsement, recommendation, or favoring by the United States Government or any agency thereof. The views and opinions of authors expressed herein do not necessarily state or reflect those of the United States Government or any agency thereof.

By acceptance of this article, the publisher recognizes that the U.S. Government retains a nonexclusive, royalty-free license to publish or reproduce the published form of this contribution or to allow others to do so for U.S. Government purposes.

The Los Alamos National Laboratory requests that the publisher identify this article as work performed under the auspices of the U.S. Department of Energy.

Los Alamos Los Alamos National Laboratory
Los Alamos, New Mexico 87545

FORM NO 836 R4
ST NO 2870 5 81

DISTRIBUTION OF THIS DOCUMENT IS UNLIMITED

111



A Chemical Precursor to Optical Damage?
Studies by Laser Ionization Mass Spectrometry

N. S. Nogar and R. C. Estler*

Chemical and Laser Sciences Division
Los Alamos National Laboratory
Los Alamos, New Mexico 87545

*Permanent Address: Department of Chemistry
Fort Lewis College
Durango, Colorado 81301

Mass spectrometry has been used in conjunction with Nomarski microscopy to characterize the initiation of optical damage in selected commercial optics. For a sample with a $\text{Al}_2\text{O}_3/\text{SiO}_2$ multilayer coating (351 nm) on a Si substrate, our results suggest layer by layer removal of the coating material with low-fluence irradiation at 1.06 μ . In addition, carbon impurities were observed in the low-damage threshold sample. For the $\text{Sc}_2\text{O}_3/\text{SiO}_2$ multilayer coated (351 nm) 7940 substrates, transient iron signals were observed at each increasing fluence level, with concomitant appearance of small circular (10 μ) pits in the surface. These pits were also associated with macroscopic damage features due to threshold testing.

Key words: optics, lasers, mass spectrometry

1. Introduction

Optical damage is often assumed to initiate by a localized absorption at chemical or physical defect sites in otherwise damage-resistant optical coatings and substrates.¹⁻³ Propagation of damage through either thermal runaway or avalanche-breakdown mechanism can be modeled once an initial source of electrons, localized high field, or thermal evaporation is identified.⁴⁻⁶ Small levels of chemical impurities including residual polishing compound and absorbing inclusions, or physical imperfections, such as grain boundaries or misoriented microcrystals, are among the candidates for initiation sites.⁷ While the participation of these source defects has long been assumed, there has been surprisingly little direct evidence to support their existence. In most previous studies, the identity and concentration of these defects was unknown, and in those cases where chemical impurities were observed, there was usually little evidence of a one-to-one correspondence between the defects and the onset of optical damage.

We report here a mass spectral study of damage in two sets of commercial optics. Mass spectroscopy has been used previously to examine the adsorption of surface contaminants on optical materials,⁸ and to characterize the dynamics of macroscopic damage events.^{9,10} In the present work, we have identified, in at least one case, a chemical contaminant associated with initiation of the damage event.

2. Experimental

In all experiments, the photodesorption/photoablation products were monitored by mass spectrometry, using one of two mass spectrometer systems. A quadrupole (QMS) apparatus was equipped with electron impact ionization, while the time-of-flight (TOF) apparatus utilized multi-photon photoionization for the production of ions. Samples examined in these experiments were commercial reflective optics of two types: $\text{Al}_2\text{O}_3/\text{SiO}_2$ multilayer coating (351 nm) on a Si substrate, and $\text{Sc}_2\text{O}_3/\text{SiO}_2$ multilayer coating (also 351 nm) on a 7940 substrate. Each sample was

secured in a holder attached to a 15-cm stainless steel rod for mounting within the mass spectrometer vacuum can. The substrates were placed near (1.5-3 cm) the source regions in both mass spectrometer systems, and were manipulated by mounting the rods on a rotation-push/pull feedthrough (Varian Model 1371). The samples could thereby be rotated so as to provide a fresh surface for exposure to the laser beam.

Nomarski micrographs were taken of the samples both before and after exposure, using a commercial microscope (Nikon). Images were recorded on Polaroid Type 53 film. A series of alignment marks on the samples were used to locate the photographed sites.

The source region of the QMS (Extrel, C-50) was equipped with an axial ionizer modified to allow a variety of laser/substrate interactions. In one configuration, the high intensity laser beam passed through the ionizer, radiating the substrate at normal incidence.¹¹ The spalled material was ejected perpendicular to the quadrupole axis. In a second geometry, the substrate was mounted on the axis of the quadrupole. The desorption laser hit the surface at a 45-degree incidence angle, ejecting the spalled material directly along the QMS trajectory axis (Fig 1). Qualitatively, both arrangements produced the same results, however, the axial configuration was several orders of magnitude more sensitive in detecting desorbed species. Primary ions produced by the damaging laser were detected by turning off the electron impact ionizer, while survey electron impact mass spectra were typically acquired at an energy of 70 eV. Ions were detected by a channel-electron multiplier, and the signal amplified and detected by a boxcar integrator (PARC 162/164) synchronized to the output of the desorption/ablation laser. Unit mass resolution is possible with this apparatus throughout the range of interest, 4-200 au. A base pressure of $\leq 1 \times 10^{-8}$ Torr was maintained in this vacuum chamber by an ion pump and/or turbomolecular pump.

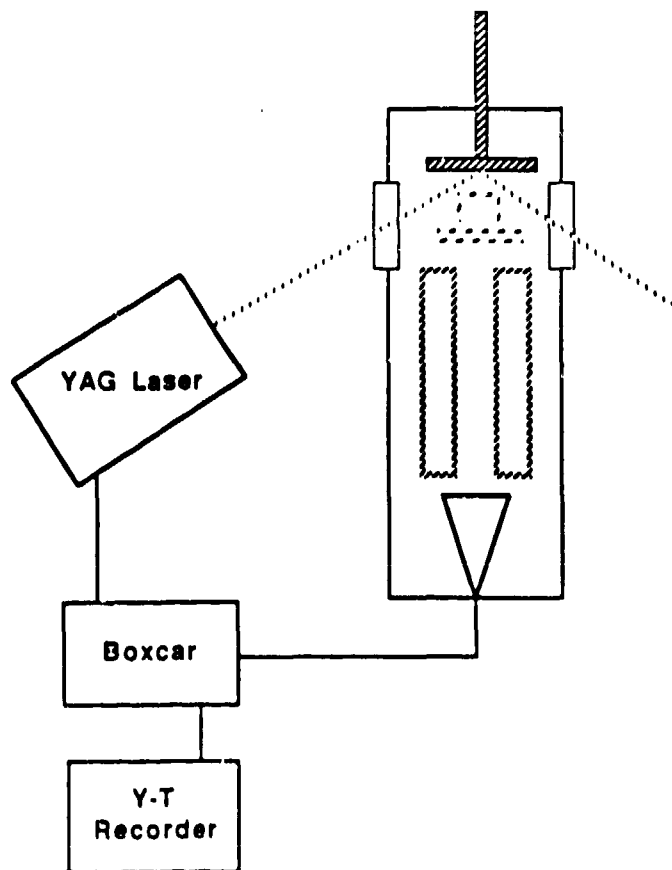


Figure 1. Experimental schematic for the "on-axis" quadrupole mass spectrometer configuration.

The source region of the TOF allowed optical access by both the desorption and interrogation laser beams.¹² Ions were again detected by a channel-electron multiplier, and the signal processed with either the boxcar integrator or transient recorder (Tektronix 2430). The latter was very important since the multiplex detection allowed acquisition of a full mass spectrum for each laser shot, and facilitated the observation of transient signals. The mass resolution of this instrument was ≈ 2 au in the range 2-200 au. A base pressure of $\leq 1 \times 10^{-7}$ Torr was maintained by a L-N₂ trapped oil diffusion pump.

Desorption/damage was initiated by the fundamental (1.06 μ) output of a Nd³⁺:YAG laser (Quanta Ray/Spectra Physics Model DCR 1A). The laser was equipped with filled-beam optics, and produced a beam whose spatial profile was somewhat more sharply peaked than for a gaussian beam. The Q-switched output was 10 ns FWHM in duration, and smooth within the resolution of our electronics (≈ 2 ns). The output of this laser was focused to a diameter of 500 μ at the front surface of the sample of interest. Beam diameters were determined by burn patterns on photographic film¹³.

The timing sequence was initiated by the Q-switch synch-out from the YAG laser. When using the quadrupole mass spectrometer, this signal triggered directly the boxcar averager gated to accept signal from laser-generated species. In experiments using the time-of-flight mass spectrometer, the YAG laser synch-out was passed through a variable delay (Tektronix 7904/7B85), a pulse generator (BNC 8010) and then to the trigger of a XeCl excimer laser (Lambda Physics EMG 101). The UV output from this laser was used to pump a tunable dye laser (Lambda Physics FL 2002) which could then probe, via multiphoton ionization, the material spalled by the laser damage event. Typical pulse energies were 1-5 mJ (12 ns FWHM) at 394 nm using the laser dye QUI (Lambda Physics). The identity of the spalled material could be determined by ion flight times and by varying the ionization wavelength, while velocity distributions could be measured by changing the delay between the damage and interrogation lasers.

3. Results and Discussion

Since the type of information obtained for the two sets of samples was qualitatively different, they shall be discussed separately.

3.1. Al₂O₃ / SiO₂ multilayer-coated Si substrate.

Two samples were examined, one having a relatively high macroscopic damage threshold (10 J/cm² @ 351 nm), while the other exhibited a low threshold (5 J/cm² @ 351 nm). Figure 2 shows typical low sensitivity mass spectra for either sample obtained with the quadrupole mass spectrometer system, and 70 eV electrons. The bottom trace is due to background gases (no sample irradiation), and exhibits small peaks corresponding to water, nitrogen, residual hydrocarbons, argon and carbon dioxide. At low fluences (1-3 J/cm² @ 1.06 μ), as damage was just beginning, results were typified by trace b, which exhibits an increase in the water-related signal (mass 16-18), and the appearance of aluminum (mass 27) and silicon (mass 28). At higher fluences (7-10 J/cm² @ 1.06 μ), or longer radiation times, the dielectric coating was removed, and a signal due primarily to bulk silicon was observed, Fig. 1c. When a higher sensitivity was used, it was possible to detect a number of other species, both ionic and neutral, in the laser generated plume (see Table I). In most experiments, the signal due to neutral species was ≥ 100 times the signal due to primary ions¹⁴ (those generated directly by 1.06 μ pulses). It is interesting to note that the carbon ions and neutrals were observed only for the low damage threshold sample, suggesting a correlation with the presence of this impurity.

Our experiments showed a factor of 10 decrease in signal for Si₂⁺ relative to Si⁺, and another order of magnitude decrease for Si₃⁺ relative to Si₂⁺. Although the large silicon clusters reported in some previous laser vaporization studies¹⁵ were not seen in this work, this is not surprising since the vaporization and expansion conditions were dramatically different. In the previous studies, the irradiation intensities were considerably higher, which should lead to a higher local density of gas phase silicon atoms, and the spalled material was expanded through a supersonic jet, which should lead to an increase in cluster formation. Both of these effects tend to skew the previously observed distributions toward higher cluster sizes.

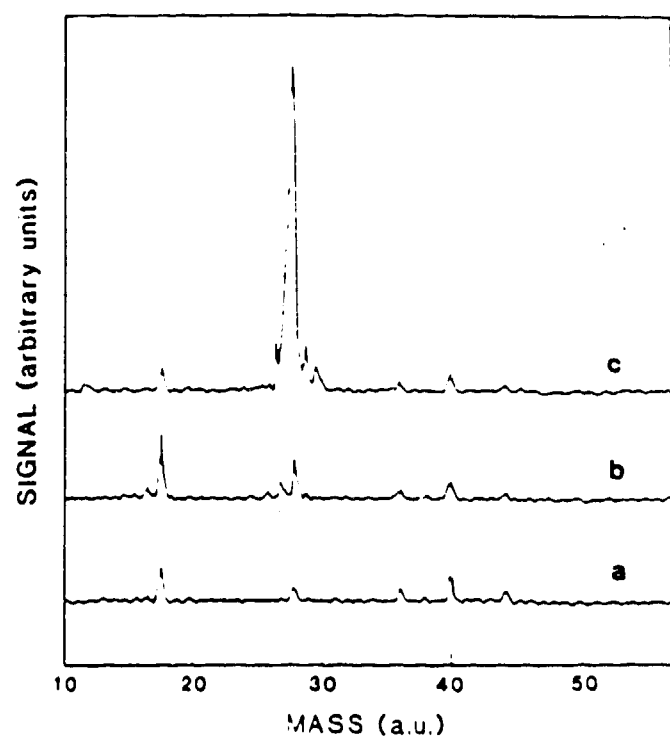


Figure 2. Low sensitivity mass spectra of laser-generated plume from $\text{Al}_2\text{O}_3/\text{SiO}_2$ multilayer coated Si substrate, obtained with 70 eV electron impact ionization. Lower trace (a) shows background gases. Trace (b) shows a characteristic spectrum for low laser fluence, while trace (c) is a typical trace for high fluence irradiation.

Table I. Ionic and neutral species observed by mass spectrometry in the laser desorption/laser ablation of coated optical samples.

Sample	Neutral Species ^a	Ionic Species ^b
$\text{Al}_2\text{O}_3 / \text{SiO}_2$ on Si	C ^c , Al, Si, SiO, Al_2O	C^+ , Si^+ , Si_2^+ , Si_3^+ , SiO_2^+ Al^+ , AlO^+ , AlO_2^+ , O_2^+ , H_3O^+
$\text{Sc}_2\text{O}_3 / \text{SiO}_2$ on 7940	Si, Sc, ScO, O_2 , $\text{Sc}_2\text{O}^\#$	Si^+ , Sc^+ , Sc_2^+ $\text{Fe}^\#$

^aRequired post-desorption ionization (laser or electron-impact) to observe by mass spectrometry
^bions produced directly in the desorption process

^cIndicates only observable in low-damage threshold sample

[#]Indicates transient signal (see text for details)

Figure 3 displays the time-dependent Al^+ signal due to 70 eV electron impact ionization of neutrals removed from the surface by laser desorption. This data was acquired at low fluence ($1.5 \text{ J/cm}^2 @ 1.06 \mu$), corresponding the onset of damage at this site. After the initial few hundred laser shots, it appears that there is some periodicity (see tick marks on the upper horizontal axis), corresponding to a period of ≈ 1200 laser shots, superimposed on a roughly exponential decay in this signal. This suggests that we may be observing layer by layer removal of the multilayer dielectric coating, although the radial growth of the damage spot may certainly be occurring concurrently. Roughly complimentary behavior was observed for the Si^+ signal (periodicity, with a phase shift relative to the aluminum signal), although for silicon, the interpretation is complicated by the 28 au background due to molecular nitrogen. In spite of this interference it was very clear from a spectacular rise in the silicon signal, with a concomitant drop in the aluminum signal, when the coatings were removed completely and the substrate material irradiated directly.

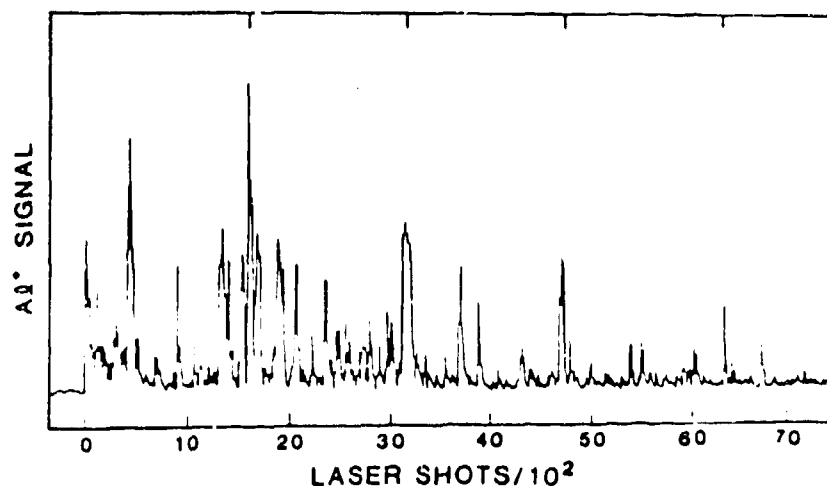


Figure 3. Time-dependent Al^+ signal generated from electron-impact ionization of plume desorbed at low fluence from the $\text{Al}_2\text{O}_3/\text{SiO}_2$ multilayer coated Si substrate. Tick marks on the upper vertical axis are coincident with periodic maxima in the signal.

3.2. $\text{Sc}_2\text{O}_3/\text{SiO}_2$ multilayer coated 7940 substrate

Table I. shows the species typically observed in the plume of material spalled from two samples (high damage threshold, $10.3 \text{ J/cm}^2 @ 351 \text{ nm}$, and low damage threshold, $3.8 \text{ J/cm}^2 @ 351 \text{ nm}$) of the $\text{Sc}_2\text{O}_3/\text{SiO}_2$ multilayer coated 7940. Those species not designated as transient were detected via 70 eV electron impact in the quadrupole mass spectrometer, and could be observed for extended periods ($\geq 10^3$ laser shots) at low fluence ($1-3 \text{ J/cm}^2 @ 1.06 \mu$) irradiation of a single site.

The "transient" species were observed only by TOF mass spectrometry, in combination with laser ionization. Figure 4 shows typical TOF mass spectra, with the lower vertical axis indicating flight time, and the upper corresponding to mass. The lower trace (a) is the (null) mass spectrum observed when the YAG laser fires, but no photons impinge on the sample. This display is the result of a four-shot average, and displays the mass range from ≈ 4 to 250 au. The deflection immediately following $t=0$ is the result of r.f.l. due to firing the ionization (excimer-pumped dye) laser. The time between firing the desorption- and excimer lasers ($\approx 14 \mu\text{s}$) was adjusted to address particles having a velocity normal to the surface of $\approx 7 \times 10^7 \text{ cm/s}$. This time delay was found empirically to maximize the observed signal.

The middle trace (b) of Fig. 4 is typical of the mass spectra observed when the desorption laser fluence is just sufficient (100 mJ/cm^2) to produce any detectable signal. In this case, the only observable signal (equivalent to 1-2 ions detected per laser shot) occurs at mass 56. Since

the ionization laser is tuned to the 5G_5 (50703.9 cm^{-1}) \leftarrow 5G_4 (0.000 cm^{-1}) two-photon transition in iron (394.4 nm), and since the observed signal is sharply peaked at this wavelength, both the mass and optical spectral signatures suggest that we are observing iron desorbed from the sample.¹⁶ It is important to note that for a particular location on the sample, this signal could only be observed for 2-6 shots at a given fluence of the desorption laser. In order to observe subsequent signal, either the location of irradiation had to be changed or the fluence raised. The uppermost trace (c) of Fig. 4 shows a signal generated at significantly higher fluence (6.4 J/cm^2). In addition to the iron signal observed in trace (b), signal is now also present at 28 au, corresponding to silicon, and at 106 au, corresponding to Sc_2O . Note that although the 28 au and 106 au signals are smaller than that observed for 56 au, this does not necessarily indicate that more iron is being removed from the surface than silicon or scandium. Since ionization is affected by a multiphoton photoionization process in which the ionization wavelength is tuned to resonance with an iron transition, the ionization efficiency is expected to be much greater (by perhaps 10^2 to 10^3) than for the non-resonant ionization of silicon- or scandium-containing fragments. Based on previous results with this apparatus,^{12,17} and the magnitude of the observed iron signal, the number of *ground state iron atoms* removed from the surface lies in the range 10^4 - 10^5 assuming the distribution is spatially isotropic and kinetically thermal. It should be noted that this does not place an upper limit on the *total* amount of material removed from these pits. Iron clusters, coating material and other impurities may be desorbed and detected with much lower efficiency than for ground state iron atoms.

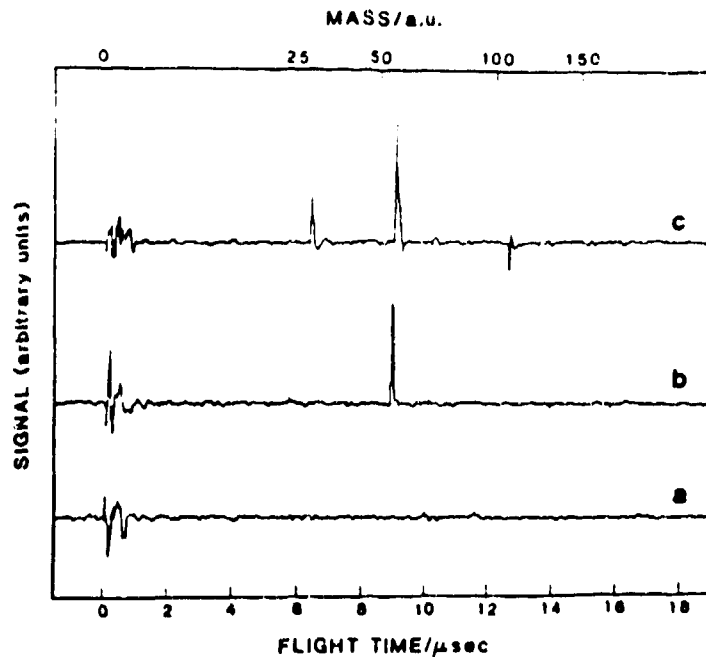


Figure 4. Time-of-flight mass spectra of laser-generated plume from $\text{Sc}_2\text{O}_3/\text{SiO}_2$ multilayer coated 7940 substrate, obtained with laser multiphoton photoionization at 394 nm . Trace (a) was generated with no plume present, and shows only r.f.i. pickup at $t=0$, when the ionization laser fires. Trace (b) displays a signal at mass 56 (Fe) due to low-fluence irradiation of the sample, while trace (c) shows additional signals at mass 28 (Si) and mass 106 (Sc_2O).

These results can be profitably compared with evidence provided by Nomarski photographs of the samples. Figure 5 displays, at 420x magnification, a section of the sample prior to laser irradiation (upper level), while the central feature shows the results of irradiation below the fluence necessary to initiate macroscopic damage. Irradiation conditions were similar to those used to obtain the mass spectrum in Fig 4b. A number round pits, approximately 10μ in diameter, can be observed within the field of view. A slight shading in the background surrounding these pits can also be observed in some instances, suggesting that some thermal deformation

occurred. Several of these circular blemishes were typically observed within the (YAG) laser footprint following experiments in which a transient iron signal was observed. In addition, the density of these pits increases with the maximum fluence to which the sample was exposed for the mass spectrometric diagnostics. Figure 5 (lower right) shows, for comparison, a macroscopic damage feature produced by an excimer laser in threshold damage testing. Several features should be noted. First, the damage test figure appears to be both larger and deeper than the circular features of 4b. And secondly, a circular feature, similar to those in 5b, can be seen to the left of center in the damage pit. In fact, for all cases in which a macroscopic damage feature was photographed, one or more of these circular features was observed within the damage footprint. In addition, each of these circular features appear to have grown from its center as marked by a deeper central damage site.

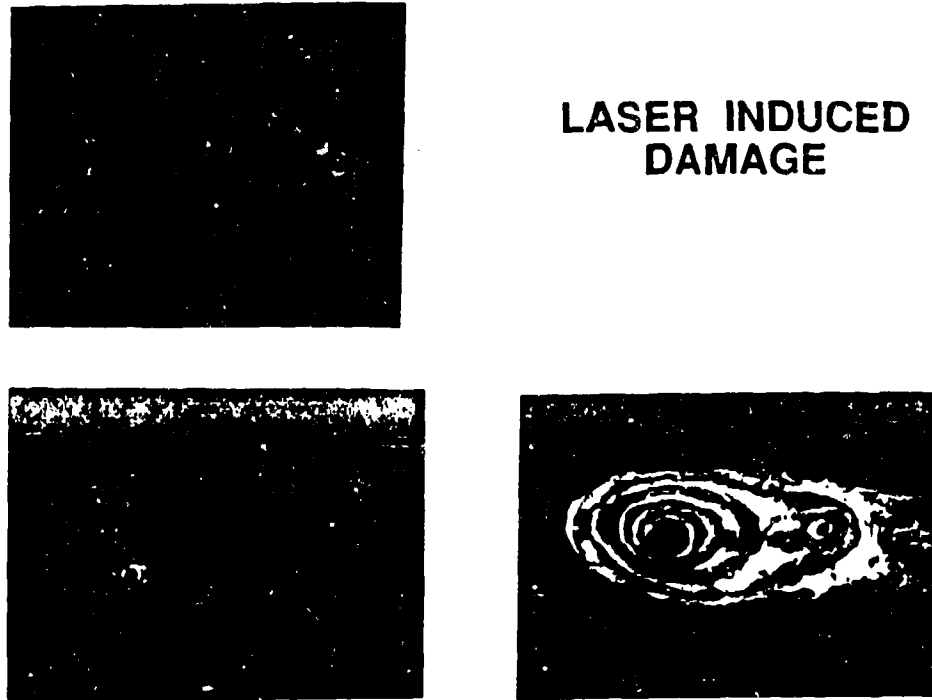


Figure 5. Nomarski micrographs (420X) of $\text{Sc}_2\text{O}_3/\text{SiO}_2$ multilayer coated 7940 substrate. Upper left shows an unirradiated surface. Lower left displays a surface subjected to low-fluence irradiation, while lower right shows a surface subjected to high-fluence irradiation, resulting in macroscopic damage.

The appearance of small pits within the irradiated area, and the concomitant detection of iron emission from the surface, strongly suggests a correlation. We believe that the observed signals are due the presence of small, iron-containing micro-inclusions in the optical coatings. Low fluence irradiation removes near-surface contaminants with minimal damage, while higher-fluence irradiation may remove more deeply imbedded, or lower susceptibility, contaminants, with concomitant removal of surrounding coating material.

This interpretation is consistent with a number of observations. In particular, previous reports^{16,19} have cited a laser-annealing effect. That is, a gradual increase in the fluence with which a sample is irradiated results in a higher measured damage threshold than for immediate irradiation at high fluences. This can be rationalized by low fluence removal of included impurities below the threshold for macroscopic damage. In addition, the association, in our experiments, of the circular pits with the macroscopic damage sites suggests that at high fluences, absorption by impurity inclusions can result in a high local temperature or field to cause macroscopic damage.

In conclusion, the combination of a method (RIMS) having high sensitivity, and good spatial and temporal resolution, with an imaging capability, such as micrography, provides a powerful tool for the study of optical damage processes. Imaging capabilities are vital, in general, for the detection of inhomogenously distributed impurities. Work is under way to introduce imaging capabilities directly into RIMS analysis.

5. References

- [1] Wood, R. M. Laser Damage in Optical Materials, Boston, Adam Hilger, 1986.
- [2] Smith, W. L. Laser-Induced Breakdown in Optical Materials. *Opt. Engin.* **17**; 489-503; 1978.
- [3] Ready, J. F. Effects of High-Power Laser Radiation, New York, Academic, 1971.
- [4] Hurt, H. H.; The Effect of Defects on the Laser Damage Performance of Metal Mirror Surfaces, Proc. 16th Ann. Symp. on Laser Induced Damage in Opt. Mat., 1984; NBS Special Publication 727; Oct. 1986, Pp. 66-70.
- [5] Siekhaus, W. J.; Kinney, J. H.; Milam, D.; Chase, L. L. Electron Emission from Insulator and Semiconductor Surfaces Below the Optical Damage Threshold, *Appl. Phys.* **A39**, 163-166; 1986.
- [6] Lange, M. R., McIver, J. K., and Guenther, A. H., Laser Induced Damage of a Thin Film with an Absorbing Inclusion: Thermal Considerations of Substrates and Absorption Profiles, Proc. 15th Ann. Symp. on Laser Induced Damage in Opt. Mat., 1983; NBS Special Publication 688; Nov. 1985, Pp. 448-453.
- [7] Johnson, L. F., Ashley, E. J., Donovan, T. M., Franck, J. B., Woolever, R. W., and Dalbey, R. Z., Scanning Electron Microscopy Studies of Laser Damage Initiating Defects in ZnSe/TiF₄ and SiH/SiO₂ Multilayer Coatings, Proc. 15th Ann. Symp. on Laser Induced Damage in Opt. Mat., 1983; NBS Special Publication 688; Nov. 1985, Pp. 356-370.
- [8] Allen, S. D.; Porteus, J. O.; Faith, W. N.; Franck, J. B. Contaminant and Defect Analysis of Optical Surfaces by Infrared Laser Induced Desorption. *Appl. Phys. Lett.* **45**; 997-999; 1984.
- [9] Estler, R. C.; Apel, D. C.; Nogar, N. S. Laser Mass Spectrometric Studies of Optical Damage in CaF₂. *J. Opt. Soc. Am. B.*, **4**, 281-286; 1987.
- [10] Levine, L. P.; Ready, J. F.; Bernal, E. G. Production of High-Energy Neutral Molecules in the Laser-Surface Interaction. *IEEE J. Quant. Elec.* **QE-4**; 18-23; 1968.
- [11] Estler, R. C.; and Nogar, N. S. Mass Spectrometric Identification of Wavelength Dependent UV-Laser Photoablation Fragments from Polymethylmethacrylate. *Appl. Phys. Lett.*, **49**, 1175-1177; 1986.
- [12] Nogar, N. S.; Estler, R. C.; and Miller, C. M. Pulsed Laser Desorption for Resonance Ionization Mass Spectrometry. *Anal. Chem.* **57**; 2441-2444; 1985.
- [13] Avizonis, P. V.; Doss, T. T.; Heinlich, R. Measurements of Beam Divergence of Q-Switched Ruby Laser Rods. *Rev. Sci. Instr.* **38**; 331; 1967.
- [14] The authors would like to thank D. A. Dahl and J. E. Delmore, EG&G Idaho, for an IBM-compatible copy of SIMION, an ion optics program which we used to estimate the relative transmission efficiencies of neutral and ionic species in our apparatus.
- [15] Heath, J. R.; Liu, Y.; O'Brien, S. C.; Zhang, Q-L; Curl, F.K.; Tittel, F. K.; Smalley, R.E. Semiconductor Cluster Beams: One and Two Color Ionization Studies of Si_x and Ge_x. *J. Chem. Phys.* **83**; 5520-5526; 1985.

- [16] Standard tests, including duplicate experiments with alternate samples and with no sample, were performed in order to insure that the iron signal originated with the sample and not from other parts of the apparatus.
- [17] Apel, E. C.; Anderson, J. E.; Estler, R. C.; Nogar, N. S.; Miller, C. M. Use of Two Photon Excitation in Resonance Ionization Mass Spectrometry. *Appl. Opt.* **26**: 1045-1050; 1987.
- [18] Frink, M. E.; Arenberg, J. W.; Mordaunt, D. W.; Seitel, S. C.; Babb, M. T.; Teppo, E. A. Temporary Laser Damage Threshold Enhancement by Laser Conditioning of Antireflection-coated glass, *Appl. Phys. Lett.* **51**: 415-417; 1987.
- [19] Franck, J. B.; Soileau, M. J. A Technique for Increasing the Optical Strength of Single-Crystal Sodium Chloride and Potassium Chloride Through Temperature Cycling, *Proc. 15th Ann. Symp. on Laser Induced Damage in Opt. Mat.*, 1981; NBS Special Publication 638; p. 114.